

# Outgassing, Temperature Gradients and the Radiometer Effect in LISA: A Torsion Pendulum Investigation

S E Pollack, S Schlaminger and J H Gundlach

*Department of Physics, University of Washington, Seattle, WA 98195-4290*

**Abstract.** Thermal modeling of the LISA gravitational reference sensor (GRS) includes such effects as outgassing from the proof mass and its housing and the radiometer effect. Experimental data in conditions emulating the LISA GRS are required to confidently predict the GRS performance. Outgassing and the radiometer effect are similar in characteristics and are difficult to decouple experimentally.

The design of our torsion balance allows us to investigate differential radiation pressure, the radiometer effect, and outgassing on closely separated conducting surfaces with high sensitivity. A thermally controlled split copper plate is brought near a freely hanging plate-torsion pendulum. We have varied the temperature on each half of the copper plate and have measured the resulting forces on the pendulum.

We have determined that to first order the current GRS model for the radiometer effect, outgassing, and radiation pressure are mostly consistent with our torsion balance measurements and therefore these thermal effects do not appear to be a large hindrance to the LISA noise budget. However, there remain discrepancies between the predicted dependence of these effects on the temperature of our apparatus.

**Keywords:** LISA, gravitational wave detectors, torsion balance, torsion pendulum, radiometer, outgassing, acceleration noise

**PACS:** 04.80.Nn, 07.10.Pz, 07.87.+v, 95.55.Ym, 91.10.Pp, 41.20.Cv

## INTRODUCTION

The low frequency end of the LISA gravitational wave sensitivity requires that the proof masses are kept in free-fall below  $\delta a = 3 \cdot 10^{-15} \text{ (m=s}^2\text{)} = \overline{\text{Hz}}$  from 0.1 to 10 mHz [1, 2, 3]. The spurious accelerations linked to random thermal fluctuations have been allocated one-third of this total budget for meeting the desired LISA sensitivity [4]. Thermal fluctuations on the electrode housing of the GRS are estimated to be  $S_{\Delta T} = 10^{-10} \text{ K}^2 = \overline{\text{Hz}}$  [2], which combined with theoretical understanding of the thermal effects yields  $\delta a_T = 3.5 \cdot 10^{-16} \text{ (m=s}^2\text{)} = \overline{\text{Hz}}$ , which is one-third of the allocation. The margin in the budget that this assessment creates could be used to relax other requirements. Therefore it is imperative that the models which were used to generate the current assessment are validated in a laboratory setting.

The three largest thermal effects in the LISA noise budget are radiation pressure, the radiometer effect, and asymmetric outgassing. These three terms add coherently: [5, 6]

$$\delta a_T = \frac{8\sigma}{3Mc} AT^3 + \alpha_P \frac{A}{2M} \frac{P}{T} + \frac{AGQ_0}{4M} \frac{\Theta}{T^2} \overline{S_{\Delta T}}; \quad (1)$$

where  $\sigma$  is the Stefan-Boltzmann constant,  $c$  is the speed of light,  $M = 1.96 \text{ kg}$  is the mass of the LISA proof mass,  $A = 2.12 \cdot 10^{-3} \text{ m}^2$  is the area of one face of the LISA proof mass,  $P = 10^{-5} \text{ Pa}$  is the residual gas pressure at the proof mass, and  $T = 293 \text{ K}$  is the temperature. The first term in Equation 1 is due to fluctuating asymmetric radiation pressure,  $\delta a_{\text{RP}}$ . The second term is due to the radiometer effect,  $\delta a_{\text{RE}}$ . The pressures on opposite faces of the proof mass equilibrate quickly so that there is nearly no pressure difference across it. This implies that the contribution due to the radiometer effect should be reduced [7]. Leading to a pressure reduction factor of  $\alpha_P = 0.1$  [8]. The last term is due to fluctuations in asymmetric outgassing on opposite sides of the proof mass. The outgassing rate  $Q(T)$  most likely will follow an exponential law in temperature referenced to an activation temperature  $\Theta$ . The value of this activation temperature should be no more than  $30000 \text{ K}$  [3]. The value for the nominal outgassing rate is taken to be  $Q_0 = 4 \cdot 10^{10} \text{ Torr L cm}^{-2} \text{ s}^{-1} = 5 \cdot 10^7 \text{ kg=s}^3$  [5]. The factor,  $G$ , is related to gas particle conductances about the proof mass and through holes in the housing walls, and to the outgassing area of the proof mass. The nominal value for LISA is  $G = 0.4 \text{ m/s}$  [5].

The derivations of these three effects were made assuming a constant temperature gradient across the housing which is then varied. This implies that the three effects described above are dependent on the frequency of fluctuations only through the level of the thermal fluctuations themselves,  $\frac{1}{S_{\Delta T}}$ .

Our apparatus provides the unique opportunity to investigate the gap spacing dependence as well as the pressure and linearity of the thermal effects. Our results are complementary to those that have been presented by the University of Trento group [6, 9]. Whereas they have designed a mock-up of the LISA proof mass and electrode housing and therefore emulate the geometry of LISA, we have an increased torque sensitivity, the ability to change the gap spacing, and a simpler geometry which allows ease in modeling [10].

## TORSION BALANCE APPARATUS

Our torsion balance apparatus is described in [10]. Each of the two halves of the copper plate has embedded a heating element and a temperature sensor. Further temperature sensors are located on the plate translation stage, near the control electrodes, on the autocollimator, on the outside of our vacuum chamber, on the inside of the styrofoam enclosure, and the temperature controlled laboratory.

We predict values for the three thermal noise sources under study for our torsion balance tests. Since our torsion pendulum measures torques we must convert the measured torques into LISA-equivalent accelerations. As mentioned in [10], this conversion is done by using a moment arm at which the spurious forces act on the pendulum and the mass of one LISA proof mass. The base pressure of our experiment is  $1.2 \cdot 10^{-5} \text{ Pa}$ . We assume that the outgassing activation temperature and the outgassing rate of copper is similar to that assumed for the LISA GRS. The cross-sectional area overlap of one half of the copper plate and our pendulum is  $A_{\text{UW}} = 4.7 \cdot 10^{-3} \text{ m}^2$ . The gas conductance rate for our setup should be similar in value to those for the LISA GRS, likewise we assume the same value for the factor  $G$ . Note that simple gas dynamics implies that the conduc-

**TABLE 1. Expected Values of Thermal Noise Sources** for LISA using the values given in the introduction, and LISA-equivalent accelerations for our apparatus using the values given in the text. The mean temperature of the copper plate and the residual gas pressure differentiates each column. The low and high pressure data were computed with base pressures of  $1.2 \times 10^{-5}$  Pa and  $1.6 \times 10^{-4}$  Pa respectively. Values in the table are in units of  $10^{-11}$  (m/s<sup>2</sup>/K)  $\sqrt{\overline{\delta a_{\Delta T}}}$ .

Noise Source		LISA	UW (25 C)		UW (28 C)	
			low pressure		high pressure	
Radiation Pressure	$\delta a_{RP}$	1.4	1.5	1.6	1.5	1.6
Radiometer Effect	$\delta a_{RE}$	0.2	0.2	0.2	2.8	2.8
Outgassing	$\delta a_{OG}$	1.4	1.3	1.2	1.3	1.2
Coherent Total	$\delta a_T$	3.0	3.0	3.0	5.6	5.6

tance rate should increase if the separation between the pendulum and plate grows, and therefore outgassing effects should decrease with plate-pendulum separation.

In Table 1 we list the predicted values for the three thermal effects in Equation (1) for LISA and the predicted values for our experiment. In this table we have computed our LISA-equivalent noise levels when the mean temperature of the copper plate in our apparatus is 298 K and when it is 301 K. From these values we predict a thermally induced acceleration noise of  $3 \times 10^{-11}$  (m/s<sup>2</sup>/K)  $\sqrt{\overline{\delta a_{\Delta T}}}$  relatively independent of the temperature of the copper plate. In addition, we show values for the system at an elevated pressure of  $1.6 \times 10^{-4}$  Pa, for which we expect an increase by nearly a factor of 2.

We present our results in terms of a thermal-to-torque transfer function. The conversion from torque to LISA-equivalent acceleration is  $15 \text{ (m=s}^2\text{)} = \text{(Nm)}$ , such that the expected thermal-to-torque transfer function should be  $2 \times 10^{12}$  Nm/K when the system is at low pressure, and about  $4 \times 10^{12}$  Nm/K for the high pressure scenario.

The copper plate reached 35 during the two day mild bakeout of our apparatus under vacuum. Our measurements were made 150 days after this bakeout occurred. The copper plate is made of oxygen-free high-conductivity (OFHC) copper, which has an outgassing rate 10 times lower than that assumed in the above calculations [11].

## THERMAL MEASUREMENTS

The temperature difference between the two halves of the copper plate emulates a *temperature gradient* across the LISA proof mass. Our procedure is to vary this gradient recording the torque, thereby the LISA-equivalent acceleration, as a function of a variety of adjustable variables, such as the temperature gradient, the mean temperature of the copper plate, the plate-pendulum separation, and the residual gas pressure inside our apparatus.

### DC Measurements

Applying constant power to the heater in either the left or right section of the copper plate shows a linear rise in temperature of that half as well as a linear response of

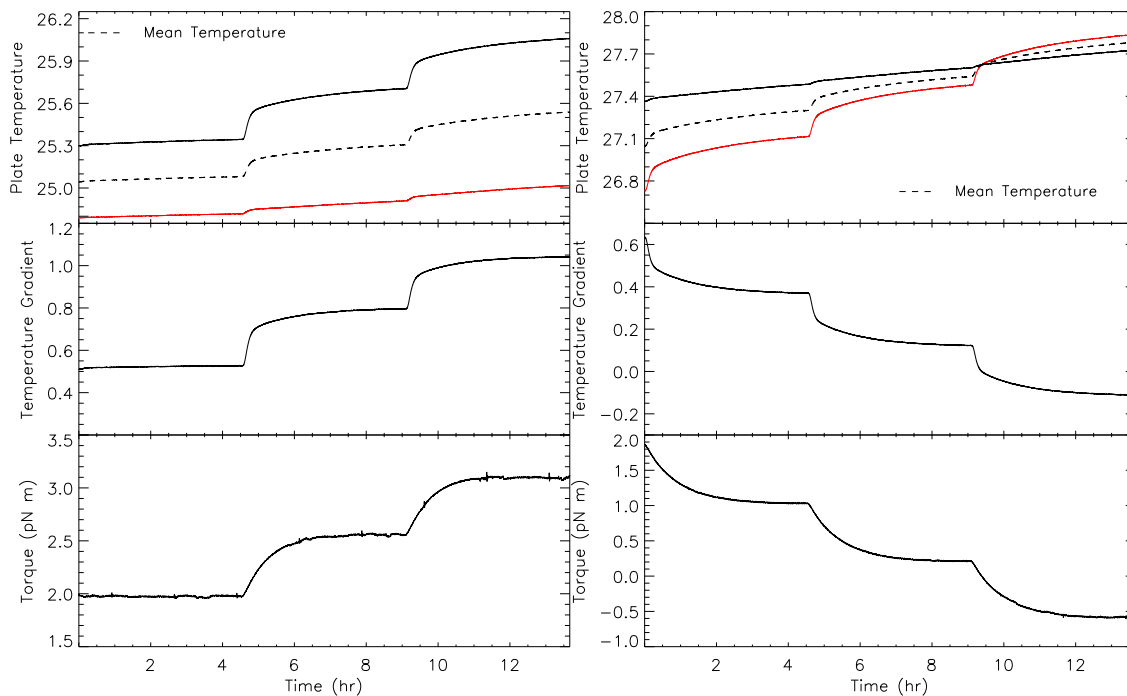


**FIGURE 1.** Heating of one half of the copper plate (left) followed by heating of the other half some time later (right) in equals steps of heater output power. The top chart shows the temperature of each half of the copper plate as well as the mean temperature all in  $^{\circ}\text{C}$ , the middle chart shows the temperature gradient between the two halves in  $\text{K}$ , and the lower chart shows the measured torque on the pendulum. The plate-pendulum separation for this data was 1 mm.

the torque on the pendulum. Figure 1 shows heating of half of the copper plate in constant steps of heater power. This data was taken with a plate-pendulum separation of 1 mm. The heated half changes by about 0.76 K over the course of this data set. Thermal coupling from one half of the copper plate to the other is 30% such that the other half gained 0.23 K. The temperature sensor placed on the electrode side of the apparatus (inside the vacuum chamber) rose by 47 mK over the course of this data set. Temperature sensors attached to the outside of the vacuum chamber changed in temperature by 46 mK. The temperature of the styrofoam enclosure did not change appreciably. This indicates that the thermal feedthrough from the copper plate to the apparatus is on the order of 10%.

It can be seen from the slower rise in the torque as compared with the temperature gradient that there is a delay between the temperature gradient and the reaction of the feedback loop of 1700 s. We suspect that this delay may be due to an effective activation time of outgassing: the trapped gas at the surface of the copper immediately escapes whereas the trapped gas within the copper slowly diffuses. Additionally, transfer of heat to the pendulum should raise the pendulum temperature by a fraction of the plate temperature change. The heating of the pendulum should increase outgassing from the silicon. There is a delay between the heating of the copper plate and the heating of the pendulum leading to a delayed response in the feedback torque.

The temperature gradient between the two halves of the split copper plate is the important quantity under investigation. The change in temperature gradient makes a change in all three thermal sources under investigation. This causes a pronounced change in the torque. The thermal-to-torque transfer function for the data on the left in Figure 1 is about 2.3 pNm/K.

After some time we heated the other half of the copper plate and brought the temperature gradient back to nearly zero. This data is on the right in Figure 1. The thermal-to-torque transfer function for this data is 3.0 pNm/K. Notice that the mean temperature of the copper plate in the data on right is 1.5 K higher than the data on the left. This increase in the transfer function appears to be a function of the mean temperature of the copper plate as described in more detail below.

## AC Measurements

The important frequency band of thermal measurements for LISA is from 0.1 to 1 mHz. Looking at coherent signals allows us to determine the thermal frequency response of our system. By sweeping in frequency from 0.1 to 1 mHz we can map the transfer function from thermal input to torque output. Figure 2 contains data for such a frequency sweep at two mean plate temperatures and two gas pressures. This data was taken with a plate-pendulum separation of 1 mm.

The thermal mass of the copper plate creates a low pass filter so that the temperature gradient amplitude is smaller at higher frequencies. Our typical amplitude is nearly 200 mK at 0.1 mHz. From a series of measurements we found that the thermal-to-torque response is independent of the signal amplitude at any particular frequency [12]. However, we still observe an apparent low pass response with a corner frequency near 0.1 mHz and a slope index of  $-0.75$  in amplitude.

From our DC measurements we found a time delay between the temperature gradient and the control torque of about 1700 s. At 10  $\mu$ Hz this would be a phase delay of  $18^\circ$  which is in good agreement with the data presented in Figure 2. This phase delay becomes larger for frequencies above 1 mHz following the decrease in transfer function. However, it appears to turn around at higher frequencies. We suspect this is an experimental artifact due to electrical coupling in our system.

To verify that this frequency and phase dependence was not dependent on our frequency sweeping function, we used a variety of different sweep functions, such as linear, logarithmic, and more complicated functions of time, as well as monochromatic sinusoids. We found no dependence on the sweep function. The individual data points in Figure 2 are for fixed-frequency sine waves.

## DISCUSSION

When the mean temperature of the copper plate is elevated by a few degrees we see an increase in the thermal-to-torque transfer function, which is not predicted by Table 1. An increase in the outgassing rate is likely the cause. As mentioned above, it is also possible that the pendulum is appreciably changing in temperature such that the outgassing rate

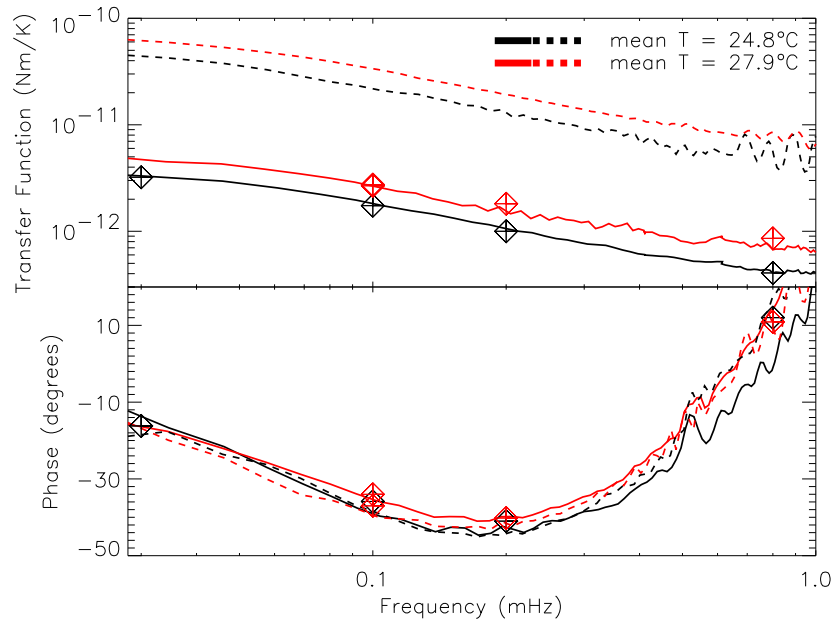


**FIGURE 2.** Thermal-to-torque transfer function and phase delay for thermal frequency sweeps between  $30\mu\text{Hz}$  and  $1\text{ mHz}$ . The solid (dashed) transfer function traces were taken at a base pressure of  $1.2 \cdot 10^{-5}\text{ Pa}$  ( $1.6 \cdot 10^{-4}\text{ Pa}$ ). Raising the gas pressure increased the transfer function by a factor of 13. Raising the mean temperature of the copper plate by  $3\text{ K}$  raised the transfer function by a factor of 1.5 irregardless of the gas pressure in our apparatus.

from the silicon increases as well. The outgassing rate should decay with time as a power law [11, 13]. Observing this decay would yield support for this hypothesis.

The radiometer effect is linearly proportional to the gas pressure in the system.

Figure 2 contains thermal-to-torque traces at an elevated pressure of  $1.6 \cdot 10^{-4}\text{ Pa}$ . The thermal-to-torque transfer function at frequencies above  $0.1\text{ mHz}$  appears to be a factor of 13 higher when the system is at this higher pressure. This linear response is exactly expected for the radiometer effect, if the radiometer effect accounted for the bulk of the thermal-to-torque transfer. As demonstrated in Table 1, the radiometer effect should be a small contribution to the total. The three contributing thermal effects add linearly since they are coherent in the temperature gradient. If outgassing and radiation pressure are independent of gas pressure, then the increase in the transfer function when the system is at high pressure would be due to the radiometer effect. This would imply that the radiometer effect is accounting for the bulk of the transfer, and therefore is a factor of 15 higher than anticipated, i.e., the pressure reduction factor,  $\alpha_P$ , should be an amplification of 1.5 not a reduction of 10. However, the radiometer effect is inversely proportional to the mean temperature and therefore does not account for the increase of 1.5 when the copper plate is at an elevated temperature.

If instead outgassing is the cause of the increase when the system is warm, then the outgassing contribution must also increase when the system is at an elevated pressure which is currently not included in the LISA models [5].

## DIRECTIONS FOR FURTHER STUDY

Our results are reasonably consistent with the current theoretical understanding of the thermal effects used in modeling for the LISA GRS. However, there does remain an anomalous increase in the thermal-to-torque transfer function when the copper plate is heated by a small amount regardless of base pressure. We are currently conducting measurements to help explain this. In addition, we are in the process of making measurements over a range of plate-pendulum separations to determine the distance dependence of the thermal effects.

## ACKNOWLEDGMENTS

We would like to thank the members of Eöt-Wash and the Center for Experimental Nuclear Physics and Astrophysics at the University of Washington for infrastructure. This work has been performed under contracts NAS5-03075 through GSFC and 1275177 through JPL, and through NASA Beyond Einstein grant NNG05GF74G.

## REFERENCES

1. P. L. Bender, K. V. Danzmann, and the LISA Study Team, *Laser Interferometer Space Antenna for the Detection of Gravitational Waves, Pre-Phase A Report*, Max-Planck Institute for Quantum Optics, Garching, Germany, 1998, MPQ-233 2nd edn.
2. A. Hammesfahr, *LISA: Study of the Laser Interferometer Space Antenna, Final Technical Report*, ESTEC contract 13631/99/NL/MS, Astrium, 2000.
3. R. T. Stebbins, P. L. Bender, J. Hanson, C. D. Hoyle, B. L. Schumaker, and S. Vitale, *Classical and Quantum Gravity* **21**, S653–S660 (2004).
4. T. Hyde, LISA Error Budget, Tech. rep., NASA GSFC, Greenbelt, MD (2005).
5. DRS ITAT, *LISA DRS Acceleration Noise Budget*, LIST Working Group 3, 2005, January 25.
6. L. Carbone, A. Cavalleri, R. Dolesi, C. D. Hoyle, M. Hueller, S. Vitale, and W. J. Weber, *Classical and Quantum Gravity* **22**, S509–S519 (2005).
7. A. Ruediger, Private communication between P. L. Bender and Albrecht Ruediger (1994).
8. R. Dolesi, D. Bortoluzzi, P. Bosetti, L. Carbone, A. Cavalleri, I. Cristofolini, M. DaLio, G. Fontana, V. Fontanari, B. Foulon, C. D. Hoyle, M. Hueller, F. Nappo, P. Sarra, D. N. A. Shaul, T. Sumner, W. J. Weber, and S. Vitale, *Classical and Quantum Gravity* **20**, S99–S108 (2003).
9. M. Hueller, L. Carbone, A. Cavalleri, G. Ciani, R. Dolesi, D. Tombolato, S. Vitale, and W. J. Weber, “Torsion pendulum investigation of thermal gradient-induced forces on LISA test masses,” in *Proceedings of the 6th International LISA Symposium*, American Institute of Physics, 2006.
10. S. Schlamminger, C. A. Hagedorn, S. E. Pollack, and J. H. Gundlach, “High Sensitivity Torsion Balance Tests for LISA Proof Mass Modeling,” in *Proceedings of the 6th International LISA Symposium*, American Institute of Physics, 2006.
11. W. G. Perkins, *J. Vac. Sci. Technol.* **10**, 543–556 (1973).
12. S. E. Pollack, S. Schlamminger, and J. H. Gundlach, *in preparation* (2007).
13. M. Li, and H. F. Dylla, *J. Vac. Sci. Technol.* **11**, 1702–1707 (1993).
14. H. Peabody, and S. Merkowitz, *Classical and Quantum Gravity* **22**, S403–S411 (2005).
15. M. Lenzen, G. M. Turner, and R. E. Collins, *J. Vac. Sci. Technol.* **17**, 1002–1017 (1999).